Brain Stimulation 13 (2020) 80–88

Contents lists available at ScienceDirect

Brain Stimulation

journal homepage: http://www.journals.elsevier.com/brain-stimulation

Direct current stimulation-induced synaptic plasticity in the sensorimotor cortex: structure follows function

Anne-Kathrin Gellner [a, b], Janine Reis [a], Carsten Holtick [a], Charlotte Schubert [a, c], Brita Fritsch [a, *]

[a] Department of Neurology, University Hospital Freiburg, Freiburg, Germany
[b] Department of Psychiatry and Psychotherapy, University Hospital Bonn, Bonn, Germany
[c] Department of Neurology, University Hospital Hamburg-Eppendorf, Hamburg, Germany

ARTICLE INFO

Article history:
Received 7 May 2019
Received in revised form
26 June 2019
Accepted 30 July 2019
Available online 1 August 2019

Keywords:
Dendritic spine
Structural plasticity
Noninvasive brain stimulation
Spine morphology

ABSTRACT

Background: Non-invasive direct current stimulation (DCS) of the brain induces functional plasticity in vitro and facilitates motor learning across species. The effect of DCS on structural synaptic plasticity is currently unknown.
Objective: This study addresses the effects and the underlying mechanisms of anodal DCS on structural plasticity and morphology of dendritic spines in the sensorimotor cortex (M1/S1).
Methods: A DCS electrode setup was combined with a chronic cranial window over M1/S1 in transgenic Thy1-GFP mice, to allow for in vivo 2-photon microscopy and simultaneous DCS. Contralateral electrical forepaw stimulation (eFS) was used to mimic the second synapse specific input, a previously shown requirement to induce functional plasticity by DCS. Changes in spine density and spine morphology were compared between DCS/eFS and sham, as well as two control conditions (sham-DCS/eFS, DCS/sham-eFS). Furthermore, the role of BDNF for stimulation-induced changes in spine density was assessed in heterozygous Thy1-GFP x BDNF+/- mice.
Results: Combined DCS/eFS rapidly increased spine density during stimulation and changes outlasted the intervention for 24 h. This effect was due to increased survival of original spines and a preferential formation of new spines after intervention. The latter were morphologically characterized by larger head sizes. The DCS-induced spine density increase was absent in mice with reduced BDNF expression.
Conclusion: Previous findings of DCS-induced functional synaptic plasticity can be extended to structural plasticity in M1/S1 that similarly depends on a second synaptic input (eFS) and requires physiological BDNF expression. These findings show considerable parallels to motor learning-induced M1 spine dynamics.

Introduction

The modulation of behavior, the phenotypical imprint of functional plasticity, by noninvasive direct current stimulation (DCS) of the brain has received increased scientific and clinical interest. In the past decade, the understanding of the underlying mechanisms of DCS including its functional synaptic effects has greatly advanced. DCS induces synaptic long-term potentiation in a motor cortex (M1) slice model, when combined with repeated, weak synaptic activation [1,2]. Moreover, anodal DCS facilitates motor skill learning in rodents and humans when combined with training [1,3–5].

Across cortical regions, functional synaptic plasticity (LTP) is causally linked with behavior (learning) on one hand [6–10] and structural synaptic changes on the other hand [11–13]. In the motor cortex, it is well documented that motor skill learning utilizes LTP as its underlying functional cellular mechanism [6] and specific dendritic spine dynamics as its structural cellular correlate in vivo [14–16]. Dendritic spines serve as the postsynaptic site of neurotransmission and respond to external and internal stimuli with experience-dependent formation, elimination and changes in morphology [6,11–13]. Induction of LTP in M1 of living rats by high frequency stimulation also increased dendritic spine density revealed by post hoc analysis [17]. Thus, translation of the volatile

* Corresponding author.
E-mail address: brita.fritsch@gmail.com (B. Fritsch).

https://doi.org/10.1016/j.brs.2019.07.026

increase in synaptic transmission into structural synaptic changes appears to be the basis for lasting cortical network remodeling, namely memory consolidation [14,15,18–20].

To date, the structural synaptic effects of DCS remain largely unknown and dynamics have not been assessed in vivo in living rodents. Post mortem, several days after intervention spine density was increased in the cortex of rats that had received repeated daily sessions of anodal DCS combined with other secondary inputs (sub- or suprathreshold for plasticity induction, e.g. auditory input, acoustic trauma or motor rehabilitative training after stroke [21,22].

Here, we assess the effects of DCS on dendritic spine dynamics of the motor cortex by longitudinal in vivo 2-photon microscopy. Since functional (LTP) and structural synaptic plasticity (i.e. dendritic spine dynamics) are positively modulated by the neurotrophin BDNF [23–27] and intact BDNF signaling is a prerequisite of DCS-induced functional plasticity and motor learning [1,28] we also highlight the role of BDNF for DCS-induced structural spine plasticity.

Materials and methods

Animals

Due to the exploratory study design both adult male and female mice (age 12.2± 1.5 weeks) with expression of enhanced green fluorescent protein (EGFP) in 10–15% of pyramidal neurons in layer 5 and more rarely layer 2/3 (Thy1-GFP M [29], Jackson Laboratory Stock #007788) were used. For experiments investigating the role of brain derived neurotrophic factor (BDNF), the Thy1-GFP M-line was cross-bred with BDNF$^{+/-}$ mice (B6.129S4-Bdnf^{tm1Jae}/J, Jackson Laboratory Stock #002266) in which BDNF expression is reduced by 50% [30]. Adult male and female Thy1-GFP x BDNF $^{+/-}$ mice aged 11.5± 2.0 weeks were used. The BDNF $^{+/-}$ genotype was verified by duplicate PCR of genomic DNA isolated from the tail. All mice were group housed under a 12:12-h light/dark cycle at constant temperature (24 °C), food and water supplied ad libitum. All animal work was performed according to the Animal Protection Law and the Directive 2010/63/EU of the European Commission. Experiments were approved by the local authorities “Commission for Animal Experimentation of the Regional Council of Freiburg” and “Commission for Animal Experimentation of the University Medical Center Freiburg” in accordance with the federal regulations.

Cranial window surgery including DCS electrode setup

For anesthesia ketamine 70 mg/kg and xylazine 20 mg/kg were given intraperitoneally. A craniotomy 3–4 mm in diameter was drilled over the primary motor and somatosensory cortex (M1/S1; coordinates approx. AP -0.5–1.5 mm and ML -1.0–3.0 mm according to Ref. [31], see also Fig. 1A–B) leaving the soft meninges intact after removal of the bone flap. A sterilized round 5 mm cover glass was equipped with a custom made circular DCS electrode (surface area 4.5 mm^2) pressed from 0.2 mm platinum wire (99.99% purity, GoodFellow, Germany, final thickness <0.05 mm) and placed onto the craniotomy leaving a thin layer of cerebrospinal fluid between the glass/DCS electrode-set-up and the meninges. The cover glass was sealed to the bone with cyanoacrylate and dental cement, which also fixed the connector of the electrode to the occipital skull. A small custom-made plastic bar was glued onto the right parietal bone used for head fixation during 2-photon microscopy to reduce movement artifacts. Carprofen 5 mg/kg body weight was applied for reduction of potential post-surgical pain and inflammation.

Assessment of the distribution of the electrical forepaw stimulation evoked cortical local field potentials in M1/S1 within the cranial window region

To confirm a synaptic input to the M1/S1 cortical region exposed to DCS and used for 2-photon microscopy the right forepaw was stimulated in three mice via 27G subdermal needle electrodes (GVB-geliMED GmbH, Germany, Fig. 1A) with pulses (0.5 mA current, 0.3 ms pulse width) generated by a Master-8 stimulator (A.M.P.I.). The evoked cortical local field potentials (LFP) were recorded with glass micropipettes filled with artificial cerebrospinal fluid (containing (in mM) NaCl 125, KCl 1.75, NaH_2PO_4 1.25, $NaHCO_3$ 25, $CaCl_2$ 2, $MgCl_2$ 1, and glucose 11) with 1–2 MΩ resistance. The cortical distribution of the evoked potentials was mapped using an Axoclamp 2A amplifier (Molecular Devices, Toronto, Canada). One microelectrode was kept in a fixed position as a reference and a second electrode was moved in 0.5 mm steps from AP -0.5–1.5 mm and ML -1.0–3.0 mm relative to Bregma using a micromanipulator. Two LFP measurements per location were performed and averaged per mouse. Mean LFP amplitudes (mV) per location were averaged across mice, transformed into a heat map and projected onto the cranial window/DCS electrode set-up (Fig. 1B).

In vivo 2-photon microscopy peri- and post stimulation

After induction of light anesthesia (ketamine 63 mg/kg, xylazine 18 mg/kg, i.p., toe pinch reflex positive) the chest was shaved, and the mouse was placed onto a 3.75 cm^2 rubber counter electrode covered with conductive gel (EMG conductive paste, GE Medical Systems). For DCS, this counter electrode and the cranial electrode were connected to a custom-built direct current stimulator (range 0–100 μA; Scientific Workshop University Neurocenter Freiburg). For electrical forepaw stimulation (eFS), two 27G subdermal needle electrodes (GVB-geliMED GmbH, Germany) were inserted subcutaneously approx. 2 mm apart on the back of the right forepaw at the level of the metacarpal bones (Fig. 1A). Body temperature was measured rectally and kept constant at 37 °C by a heating mat connected to a closed loop temperature controller (TCAT-2LV Controller, Physitemp, Clifton, NJ, USA). The head was fixed under the ocular using a custom-made holder (Scientific Workshop University Neurocenter Freiburg). A confocal microscope setup (Olympus Fluoview1000, Olympus, Germany) equipped with a Ti-sapphire laser (MaiTai HP, Spectra Physics, Germany) and water immersion objective lens (25x, NA 1.05, Olympus, Germany) was used for 2-photon microscopy. Excitation wavelength was tuned to 910 nm for imaging of EGFP positive dendritic spines. The imaging position within the cranial window was based on the availability of dendrites meeting the requirements for imaging and analysis as follows: Image stacks (50 slices) of a region with at least four dendritic segments suitable for separate analysis in the dendritic tuft of layer 5 pyramidal cells, 20–100 μm below the pial surface, were captured consecutively every 10 min at a resolution of 0.09 μm/pixel (x, y) and 0.88 μm (z-step) and at a scanning speed of 20–40 μs/pixel. The average stack acquisition time was 5.09 or 9.67 min, depending on scanning speed. Both photomultiplier tubes settings and excitation power were kept constant during time-lapse imaging.

At 0 min a first stack (baseline) was acquired. Consecutively, at 10 min, recording of the second stack was started with onset of the 20 min DCS and eFS stimulation period. Acquisition of stack 3 was started at 20 min (in the middle of the stimulation period), stack 4 started immediately after the end of stimulation (0 min post). Stack 5 started 10 min post stimulation. The same region of interest was revisited after 24 h for a second 2-photon microscopy session

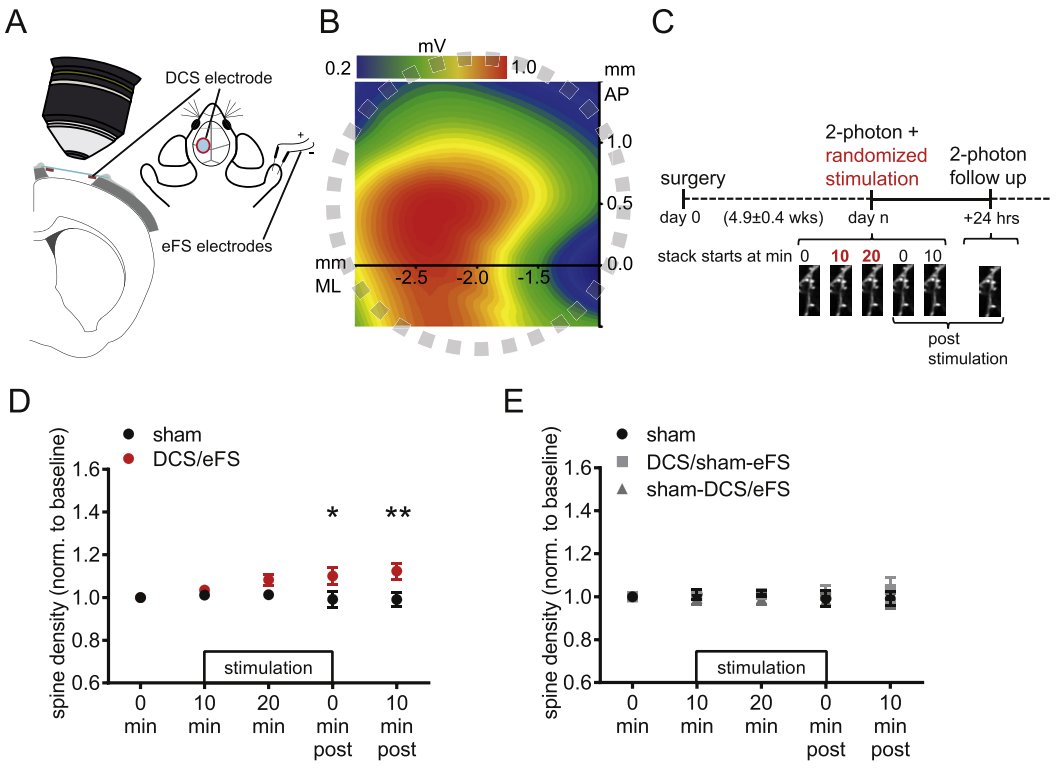

Fig. 1. Anodal direct current stimulation (DCS) rapidly increases dendritic spine density in the sensorimotor cortex in vivo when combined with electrical forepaw stimulation (eFS). (A) Schematic setup for combined DCS and eFS during 2-photon microscopy of cortical dendritic spines. The chronic cranial window is equipped with a circular platinum electrode (red) attached to the bottom of the cover glass (blue), positioned above the left sensorimotor cortex (M1/S1). 20 min of DCS (0.0 (sham) or 2.2 A/m^2) is applied while the contralateral forepaw is electrically stimulated simultaneously (0.0 (sham) or 0.5 mA at 0.1 Hz). (B) Distribution of the averaged local field potential (mV, n = 3, co-ordinates relative to bregma) generated by eFS within the margins of the projected DCS electrode (grey dashed circle) above the left M1/S1. (C) Timeline of the experiment including microscopy directly before, during and after stimulation for immediate DCS effects and follow up microscopy one day later for delayed effects. (D) Immediate DCS effects: DCS/eFS rapidly increases spine density during and after stimulation compared to sham, the difference is significant immediately after intervention. (sham: 35 dendrites/7 mice with a total of 1142 μm of dendrite analyzed; DCS/eFS: 28 dendrites/6 mice with a total of 1054 μm of dendrite analyzed). (E) DCS/sham-eFS and sham-DCS/eFS fail to induce changes in spine density compared to sham (DCS/sham-eFS: 40 dendrites/7 mice with a total of 1146 μm dendrite analyzed; sham-DCS/eFS: 30 dendrites/6 mice with a total of 1034 μm dendrite analyzed). Data shown as mean ± SEM; *p < 0.05, **p < 0.01. (For interpretation of the references to colour in this figure legend, the reader is referred to the Web version of this article.)

(Fig. 1C). The combination of either 20 min of anodal DCS at 0.0 (sham) or 2.2 mA/m^2 combined with 20 min of eFS at 0.0 (sham) or 0.5 mA at 0.1 Hz with a pulse duration of 0.3 ms generated by a Master-8 stimulator (A.M.P.I.) resulted in four different stimulation conditions. Stimulation groups were referred to as DCS/eFS, DCS/sham-eFS, sham-DCS/eFS or sham. In the "sham" condition the current applied cranially and to the forepaw was 0.0 mA. The anodal DCS stimulation intensity of 2.2 mA/m^2 was chosen for two reasons: first, it is close to intensities used in human applications and second, it is far below the threshold for microglia or astrocyte activation (15.9 A/m^2) or neurodegeneration in rodents [32]. During DCS current flow was constantly monitored using an amperemeter. After imaging sessions, mice were monitored in a warming box until fully recovered and then returned to their home cages.

Image analysis

Fiji was used for image processing and analysis [33]. Image stacks were deconvoluted using the Deconvolution Lab plugin [34] and corrected if needed to achieve equal brightness/contrast conditions compared to the baseline image for all time points of an experiment. In the baseline stack 4–8 dendritic sections were defined for repeated analysis. Spines were evaluated and counted per protocol [35] at every timepoint. Length, head and neck diameter of spines were assessed manually in the stack at baseline and at 24 h to classify morphology as described elsewhere [36]. The spine density was calculated for each animal as the total number of spines per total length of the analyzed dendritic segments. Since spine density was variable across mice, normalized spine density (relative to baseline) was used for graphical display and analysis, unless stated otherwise. Spines present at baseline were termed "original spines" and the survival fraction was expressed as percentage of original spines still present at 24 h post stimulation. Moreover, the density of new spines (not present in the stack 10 min post stimulation but present in the stack at 24 h), lost spines (present in the stack at 10 min post stimulation but not at 24 h) and stable spines (present in the two stacks 10 min post stimulation and 24 h later), was calculated to further dissect the spine turnover contributing to delayed stimulation effects. These parameters were normalized to the dendritic length (/10 μm) and absolute changes in spine density were calculated.

Statistical analysis

Given the exploratory design of the study, no statistical methods were used to estimate sample sizes a priori. Statistical analyses were performed in GraphPad Prism Version 6.01. The value of n represents the number of mice undergoing 2-photon microscopy.

Data are presented as mean ± SEM. All data distributions were tested for normality using the Kolmogorow-Smirnov test. Depending on the outcome, parametric (two-sided unpaired *t*-test) or nonparametric tests (Mann-Whitney-U-test) were used for group comparisons. Separate repeated measures analyses of variance (ANOVA) were used to assess the effect of time and electrical stimulation paradigm as well as their interaction on spine density in each stimulation condition compared to sham. In case of significant differences in the ANOVA, post hoc analysis for each time point was carried out using uncorrected t-tests. Mice that underwent cranial window surgery were excluded prior to the collection of experimental data in case of low imaging quality (e.g. blurring of the cranial window). No post hoc exclusions were made. Sex was not an independent factor in this exploratory study.

Results

Integration of the DCS electrode into the chronic cranial window set-up allowed for longitudinal 2-photon in vivo microscopy even during DCS (Fig. 1A). We assessed acute (day n) and delayed effects (day n+24 h) of DCS on dendritic spine dynamics in the M1/S1 region (Fig. 1 C). Our previous results from slice and human experiments [1] emphasized the need for repeated synaptic coactivation during DCS to evoke LTP or improvements in performance. Hence, electrical stimulation of the contralateral forepaw was used to establish a synaptic input to the same cortical area that was assessed by 2-photon microscopy and targeted by DCS (Fig. 1A and B). 4.9 ± 0.4 weeks post-surgery Thy1-GFP mice were assigned randomly to one of four stimulation conditions (sham, DCS/eFS, DCS/sham-eFS or sham-DCS/eFS). Subsequently, mice underwent additional sessions (i.e. the other stimulation conditions), separated by at least 5 days to avoid carry-over effects. The order of sessions followed a predefined balanced crossover protocol. Study duration per mouse was restricted by the age of the mouse (mature adult state, cut-off for last imaging session: week 40), the quality of the cranial window and the availability of the 2-photon microscope. Each mouse underwent at least one session. The average no. of sessions was 2.4 ± 0.4 sessions per mouse.

Immediate stimulation effects

At t = 0 min (baseline), spine density was identical in the sham group and the DCS/eFS group (both 2.8 ± 0.3 spines/10 μm, $t(11) = 0.022$, $p = 0.6537$, for all groups see SFig. 1). As can be seen in Fig. 1D, spine density started to increase over the 20 min period of DCS/eFS and further increased in the following 10 min post DCS compared to sham (STIMULATION x TIME interaction, $F4,44 = 3.502$, $p = 0.0144$, sham: n = 7, DCS/eFS: n = 6). There was a significant effect of STIMULATION ($F1,11 = 6.619$, $p = 0.0259$) but not TIME ($F4,44 = 2.383$, $p = 0.0658$). Post hoc tests revealed a significant difference between the sham and the DCS/eFS group at 0 min post stimulation (99.12 ± 3.7% versus 110 ± 4.2%, $t = 2.9159$, $p = 0.0051$) and at 10 min post stimulation (99.03 ± 3.2% versus 112.4 ± 3.8%, $t = 3.5647$, $p = 0.0007$). In contrast spine density was neither affected by DCS/sham-eFS [TIME: $F4,48 = 0.1371$, $p = 0.9678$, STIMULATION: $F1,12 = 0.09650$, $p = 0.7625$, interaction $F4,48 = 0.2927$, $p = 0.8813$, n = 7, Fig. 1E] nor by sham-DCS/eFS [TIME: $F4,44 = 0.3524$, $p = 0.8410$, STIMULATION: $F1,11 = 0.1402$, $p = 0.7152$, interaction $F4,44 = 0.9712$, $p = 0.9828$, n = 6, Fig. 1E].

Delayed stimulation effects

On the following day (day n +24 h) the spine density was significantly higher in mice treated with DCS/eFS (116.9 ± 5.4%, n = 6) compared to sham (94.48 ± 3.4%, n = 7, $t(11) = 3.644$, $p = 0.0039$, Fig. 2A and B). Moreover, spine density in the DCS/eFS condition was approximately 4% higher than on day n, pointing towards an outlasting stimulation effect on changes in spine density. In accordance with the results regarding immediate stimulation effects, neither DCS/sham-eFS (n = 7) nor sham-DCS/eFS (n = 6) affected spine density compared to sham ($t(12) = 0.7936$, $p = 0.4429$ and $t(11) = 0.3885$, $p = 0.7051$, respectively, Fig. 2A).

In more detailed analyses, we found that DCS/eFS (n = 6) favored the survival of original spines present at baseline compared to sham (n = 7: $t(11) = 2.433$, $p = 0.0332$, Fig. 2C). To further dissect the spine turnover that had occurred between 10 min post stimulation and 24 h the fraction of new, lost and stable spines was explored. Relative to sham, DCS/eFS significantly increased the density of new spines ($t(11) = 2.375$, $p = 0.0368$, n = 7 and 6, respectively, Fig. 2D), while lost spines remained unchanged ($t(11) = 0.7478$, $p = 0.4703$, Fig. 2E). There was a slight trend towards a higher density of stable spines after DCS/eFS ($t(11) = 1.842$, $p = 0.0925$, Fig. 2F). As expected, DCS/sham-eFS (n = 7) and sham-DCS/eFS (n = 6) did not alter survival of original spines compared to sham (n = 7: $t(12) = 0.1809$, $p = 0.8595$ and $t(11) = 0.4951$, $p = 0.6303$, respectively, SFig. 2A**).** Moreover, dynamics of new, lost and stable spines in these groups did also not differ from sham (new/lost/stable spines: DCS/sham-eFS (n = 7): all $t(12) > 0.5433$, $p > 0.5$; sham-DCS/eFS (n = 6): all $t(11) > 0.5426$, $p > 0.5$,SFig. 2B–D).

Changes in spine morphology by combined DCS and eFS

Since changes in spine morphology (e.g. enlargement or shrinkage) are linked to distinct roles for functionality and strength of synaptic transmission [19,37], spines were categorized into three classes: mushroom and stubby spines with distinguishable heads or thin, headless spines. Their relative contribution to the observed delayed stimulation effects on spine density (Fig. 2A) was assessed by comparing changes in spine density between baseline and 24 h post DCS/eFS or sham for each of the three spine types separately (for absolute densities of mushroom, thin and stubby spines at baseline and 24 h please see SFig. 3). As can be seen in Fig. 3A, the absolute change of spine density at 24 h after DCS/eFS (n = 6) compared to sham (n = 7) was slightly enhanced in mushroom spines ($t(11) = 1.942$, $p = 0.0782$) and significantly enhanced in stubby spines ($t(11) = 2.269$, $p = 0.0444$, Fig. 3A). The change in thin spine density remained unaltered by DCS/eFS ($t(11) = 0.4246$, $p = 0.6793$, Fig. 3A). Since the higher spine density in the DCS/eFS condition at day n + 24 h was driven by significantly increased density of new spines that occurred between 10 min and 24 h post stimulation (Fig. 2D), changes in this spine fraction was also compared to sham regarding spine morphology. The absolute change of new spine density at 24 h after DCS/eFS (n = 6) compared to sham (n = 7) was significantly higher in spines with distinguishable heads (mushroom spines $U = 7.000$, $p = 0.0449$; stubby spines $t(11) = 2.653$, $p = 0.0224$, Fig. 3B) without a difference for thin, headless spines ($U = 20.00$, $p = 0.7308$).

Potential contribution of BDNF to stimulation-driven changes in spine density

To gain further mechanistical insight into the DCS/eFS-driven effects on structural synaptic plasticity, the potential contribution of BDNF was assessed by exposing Thy1-GFP x BDNF $^{+/-}$ mice to DCS/eFS or sham under the same experimental procedures as in the main experiment (start of 2-photon microscopy 5.1 ± 0.4 weeks post-surgery, 1.8 ± 0.2 sessions per animal). Given the lack of effects in the main experiment, DCS/sham-eFS and sham-DCS/eFS was not applied in this experiment. At baseline, spine density was similar in the Thy1-GFP x BDNF $^{+/-}$ mice (3.3 ± 0.2/10 μm, n = 14) compared

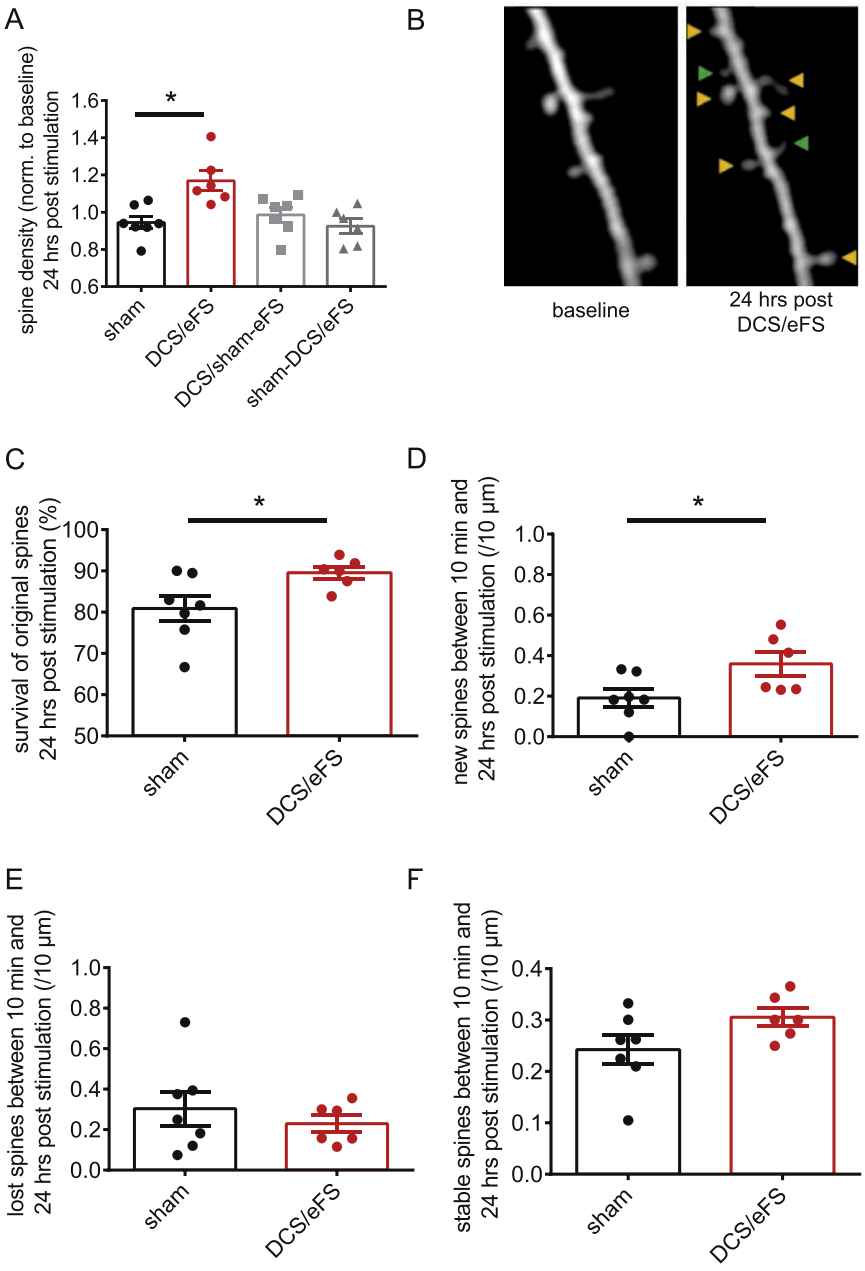

Fig. 2. Delayed effects of combined DCS and eFS on dendritic spines (A) 24 h post stimulation spine density is significantly increased in the DCS/eFS group relative to sham. As expected, no delayed effects are visible in the two control conditions (DCS/sham-eFS, sham-DCS/eFS). (B) Illustrative image of a dendritic segment with original spines (yellow arrow heads) preserved from baseline and spines gained between baseline and 24 h after DCS/eFS (green arrow heads). (C) Compared to sham, DCS/eFS leads to a significantly higher survival rate of original spines that were present at baseline. (D) Density of new spines that appeared between 10 min post stimulation and 24 h later is significantly higher in the DCS/eFS group compared to sham. (E) DCS/eFS does not affect the loss of spines per µm dendrite between 10 min post stimulation and 24 h. (F) DCS/eFS non-significantly increases the density of stable spines between 10 min post stimulation and 24 h later compared to sham. sham (35 dendrites/7 mice with a total of 1142 µm of dendrite analyzed; DCS/eFS: 28 dendrites/6 mice with a total of 1054 µm of dendrite analyzed; DCS/sham-eFS: 40 dendrites/7 mice with a total of 1146 µm dendrite analyzed; sham-DCS/eFS: 30 dendrites/6 mice with a total of 1034 µm dendrite analyzed). Data shown as mean ± SEM; *$p < 0.05$, **$p < 0.01$. (For interpretation of the references to colour in this figure legend, the reader is referred to the Web version of this article.)

to the Thy1-GFP mice used in the main experiment (2.8 ± 0.2/10 µm, $n = 13$: $t(25) = 1.818$, $p = 0.0811$, Fig. 4A). In the Thy1-GFP x BDNF $^{+/-}$ mice, DCS/eFS decreased spine density compared to sham immediately after stimulation (TIME: $F4,48 = 3.118$, $p = 0.0233$, GROUP: $F1,12 = 5.002$, $p = 0.0451$, interaction: $F4,48 = 4.694$, $p = 0.0028$, $n = 7$ per group, Fig. 4B). Post hoc tests showed significant group differences at 0 min and 10 min after stimulation ($t = 3.2335$, $p = 0.002$ and $t = 3.5719$, $p = 0.0007$, respectively, Fig. 4B). Delayed effects were not observed, since spine density was similar in both groups 24 h post stimulation ($t(10) = 0.7813$, $p = 0.4527$, sham $n = 5$, Fig. 4C).

Discussion

Using in vivo time-lapse 2-photon microscopy of dendritic spines we demonstrate immediate induction and persistence of

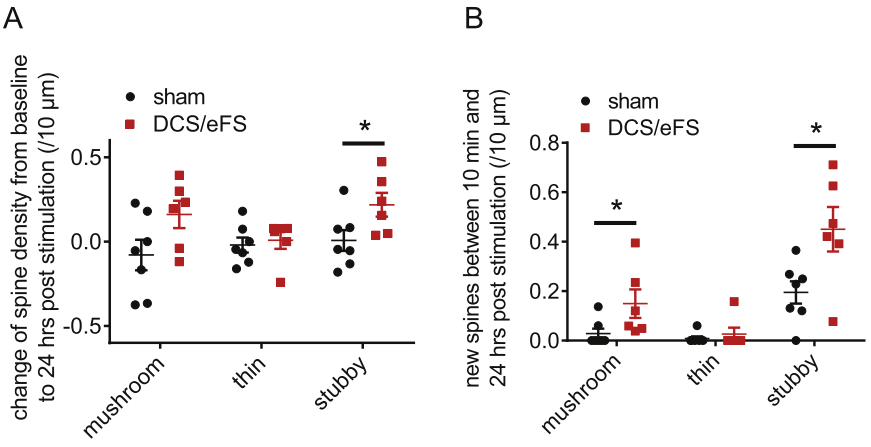

Fig. 3. Spine morphology is shifted by combined DCS and eFS towards bigger headed spines. (A) DCS/eFS increases spine density of mushroom and stubby spines from baseline to 24 h post stimulation, but spine density remains unchanged in thin, headless spines. Compared to sham, this increase is significant after DCS/eFS for stubby spines. (B) In comparison to sham, DCS/eFS significantly enhances spine density of new mushroom spines and new stubby spines, that appeared between 10 min post stimulation and 24 h later. Thin spines are not affected by DCS/eFS compared to sham. Data shown as mean ± SEM; *p < 0.05.

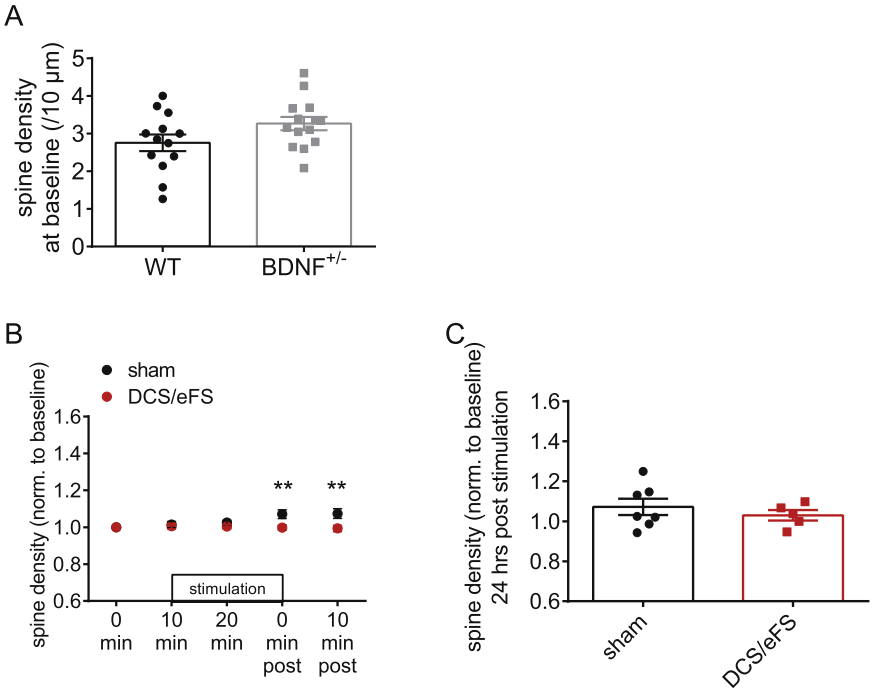

Fig. 4. Combined DCS and eFS does not enhance dendritic spine density in mice with reduced expression of brain derived neurotrophic factor (BDNF). (A) M1/S1 spine density is similar in Thy1-GFP wildtype and Thy1-GFP BDNF $^{+/-}$ mice at baseline. (WT: 63 dendrites/13 mice with a total of 2196 µm of dendrite analyzed; BDNF$^{+/-}$: 70 dendrites/14 mice with a total of 2766 µm of dendrite analyzed). (B) In BDNF $^{+/-}$mice DCS/eFS does not increase spine density. Instead, a significant decrease is seen immediately after DCS/eFS compared to sham. (Sham: 35 dendrites/7 mice with a total of 1428 µm of dendrite analyzed; DCS/eFS: 35 dendrites/7 mice with a total of 1338 µm of dendrite analyzed) (C) Spine density does not differ between groups 24 h after stimulation, suggesting a lack of a delayed stimulation effect. (Sham: 35 dendrites/7 mice with a total of 1428 µm of dendrite analyzed; DCS/eFS: 25 dendrites/5 mice with a total of 924 µm of dendrite analyzed). Data shown as mean ± SEM; **p < 0.01.

M1/S1 cortical structural synaptic plasticity by a single session of anodal DCS in combination with a repeated low frequent synaptic input (electrical forepaw stimulation). This effect depends on physiological BDNF expression.

DCS/eFS mediated a rapid increase in spine density in M1/S1. This increase started already during stimulation and continued further immediately after stimulation, up to at least 24 h later. It is important to note, that the stimulation parameters used for the DCS/eFS intervention are considered to elicit or promote physiological activity without inducing cellular damage or inflammatory responses [32]. Therefore, the rapid change in spine density observed here is clearly distinguishable from changes induced by excessively high synaptic network activity (e.g. a seizure) or acute brain injury such as a stroke [22,38,39].

Our data extent our and others work reporting the rapid induction and maintenance of functional synaptic plasticity (DCS-

LTP) in a M1 slice preparation by anodal DCS, when combined with low frequent synaptic activation [1,2]. In accordance, spine density was only enhanced by combined DCS/eFS but not sham-DCS/eFS or DCS/sham-eFS. It is thus tempting to speculate that a higher excitability by anodal DCS may increase the likelihood of timely coupled pre- and postsynaptic firing when combined with a repeated subthreshold activation of a specific subset of synapses by low frequency afferent stimulation. Consequently, both functional and structural synaptic plasticity may be promoted, in line with the concept of spike-timing-dependent plasticity [40,41]. In our experiments the synapse-specific activation co-applied with DCS is subthreshold, i.e. not sufficient to independently induce functional and structural plasticity. There is also the case in which a suprathreshold stimulus induces a specific form of plasticity, that is modified in its induction or extent by DCS, e.g. in the case of motor skill learning. Across species, anodal DCS applied to the motor cortex enhances motor skill learning [1,3,4], with the most robust effects achieved when DCS and training are timely coupled [1,3,4].

Structural synaptic DCS effects under physiological conditions have not been investigated longitudinally in vivo so far. In a different cortical region, anodal DCS combined with an auditory input (noise of 40 db, constituting a constant subthreshold input) elicited increased auditory cortex spine density assessed ex vivo in normal-hearing rats [21]. Moreover, anodal DCS also increased spine density analyzed ex vivo in acoustic trauma induced deafferented auditory cortex (with the trauma representing a suprathreshold stimulus for altered spine dynamics). It should be noted that these experiments assessed long-term effects 30 days after intervention and immediate effects were not investigated.

A physiological context in which rapid functional and structural synaptic plasticity occurs in M1 is motor learning. On the functional level, LTP is occluded in M1 after repeated sessions of motor skill learning, supporting the view that strengthening of synaptic connections is the cellular correlate of learning [6]. Improved performance is associated with a remodeling of cortical movement representations and a refinement of task-specific motor networks in humans [42,43] and rodents [44,45]. On the structural synaptic level, an initial increase in total spine number (or spine density) in superficial layers of M1 in the early days of learning is followed by increased spine elimination, leading to similar net spine density as in the pre-trained stage, but a different connectivity pattern [14,15,46]. It is conceivable that successive improvements in task proficiency are the result of the structural reorganization of a refined task specific neuronal network [14,15,46], which in the later stages of learning occur even independent of ongoing training [46]. While the time course studied in these motor learning experiments is longer than the time course of our assessment of DCS/eFS effects, similarities with regard to the early time course of spine formation and elimination in M1 after motor learning can be found: New spine formation is doubled as early as one hour after a single skilled reaching training and remains elevated for several days of training [14]. This effect depends on learning of a specific task, not forelimb movement in general, and the percentage of early spinogenesis correlates with learning success [14]. It is thus conceivable that the experience-dependent expression of new spines provides the basis for new memory formation and retention allowing for information storage in stable but modifiable networks [14,15]. Moreover, it can be assumed that the occurrence of new spines in response to activation of identical specific synaptic connections [6] is input-specific, in line with the concept of synapse-specificity of functional plasticity (LTP) [47]. Spine elimination does not contribute to initial learning, but seems to represent a hallmark of later training ($>/=2$ days), contributing to stable or reduced net spine density [14,15,46]. Twenty-four hours after stimulation, spine density remained higher in the DCS/eFS condition compared to sham. Therefore, we wished to clarify which changes in specific spine fractions contributed to the enhanced net spine density, i.e. suggesting a network remodeling effect of DCS/eFS. Indeed, the lasting effect of DCS/eFS was based on enhanced survival of original spines and a higher fraction of spines formed newly between 10 min and 24 h post stimulation. Spine elimination was not altered, and stable spines remained unchanged by DCS/eFS. It is thus arguable that the stimulation applied on day n triggered an ongoing network reorganization outlasting the stimulation period and upholding at least until the next day, mimicking the physiological changes occurring during early motor learning. While stimulation effects exceeding the 24 h post stimulation time window were not in the focus of this study, it is tempting to speculate that spine elimination may occur at later time points or the longevity of newly formed spines may be positively affected by DCS/eFS. The latter is supported by our morphological analysis, since spine head size is an indirect indicator for the longevity and strength of a synaptic connection [18–20,37,48,49]. Mushroom and stubby spines with distinguishable heads display a higher probability of longevity and strong synaptic transmission due to greater expression of AMPA receptors [19,20,37,50], with mushroom spines exhibiting the highest chance of long-term stability, serving as a potential building block for long-term memory storage [50]. Indeed, we found a higher density of stubby and mushroom morphology specifically in new spines formed between 10 min and 24 h after DCS/eFS, providing a first hint towards a potentially long-lasting network remodeling by DCS/eFS, which requires confirmation in future studies. Taken together, the specific alterations of spine dynamics and spine morphology up to 24 h post stimulation indicate that DCS/eFS bears the potential of real structural network shaping and mimics dynamics of physiological early motor learning related network reorganization.

Finally, we clarified the potential contribution of BDNF to the DCS/eFS-induced effects on structural plasticity. We did not observe baseline differences in M1/S1 spine density in Thy1-GFP x BDNF $^{+/-}$ mice, in accordance with others [26,51,52]. On the functional synaptic level, the physiological properties of DCS-LTP require intact BDNF secretion and TrkB receptor activation [1,28]. Moreover, motor learning is not significantly improved by anodal DCS when BDNF secretion is impaired [1], which is consistent with the role of BDNF in functional and synaptic plasticity and learning [23,53]. Translation of volatile increases in synaptic strength to solid structural connectivity changes has been related to successful memory consolidation [12,14,15,18,19]. Hence, impairment of functional synaptic plasticity alone by reduced BDNF signaling may partially explain both the behavioral deficits in BDNF deficient conditions as well as potentially impaired structural connectivity. In accordance, altered spontaneous spine dynamics may already be present under sham conditions. Here, the increase in spine density by DCS/eFS observed in wild type mice was not present in the Thy1-GFP x BDNF $^{+/-}$ mice. In fact, even a short-lasting reduction in spine density occurred, that did not prevail 24 h later. This brief decrease in spine density may rely on reported altered receptor expression [54] or altered activity-dependent action on the actin cytoskeleton [27] in BDNF $^{+/-}$ mice.

With regard to spine morphology, BDNF signaling modulates short lasting activity-dependent spine head size changes and promotes larger spine head sizes in the adult visual cortex [55]. In line with these findings the DCS/eFS effects on spine morphology (specifically promotion of larger spines with distinguishable head sizes, but not thin spines) also suggests a mechanistical role of BDNF. So far we cannot differentiate whether deficient functional synaptic plasticity in these mice [1,56,57] - here DCS-LTP - hinders the subsequent structural synaptic plasticity or whether BDNF-

dependent downstream mechanisms in the translation from functional to structural plasticity might be affected additionally.

Limitations

In the current study we did not address how the neuronal network structural changes develop beyond 24 h post stimulation. Hence, it remains unknown whether enhanced survival of DCS/eFS derived new spines occurs in concert with delayed elimination of older spines as seen with physiologically driven spine dynamics, e.g. after motor learning [14,15]. Future studies should include extended time courses of structural plasticity to resolve this question. From an experimental standpoint, we established an artificial synaptic input (eFS) for co-application with DCS in lightly anesthetized mice. For translational reasons, the implementation of a behaviorally or rehabilitation relevant task instead of eFS may allow to study the whole process of network reorganization on the synaptic level in a more real-life scenario. However, motor skill learning is performed in alert animals, constituting a practical challenge for in vivo 2-photon microscopy in concert with DCS.

Conclusion

Taken together, this study provides evidence for specific DCS/eFS-induced structural synaptic plasticity in M1/S1 in vivo that depends on a second synaptic input and requires intact BDNF expression. These findings show considerable similarities to motor-learning induced M1 spine dynamics and strongly support the previously observed effects of DCS on functional synaptic plasticity.

Declarations of interest

None.

Funding

This work was supported by the German Research Foundation (RE2740/3-1).

Acknowledgements

We thank Marco Prinz and his group members for access to and support with the 2-photon microscope, Carola Haas for provision of Thy1-GFP M mice, and Juliane Schiweck and Nahid Kuhenuri Chami for help with data analysis. We also thank Gerd Strohmeyer and Frank Huethe from the Scientific Workshop of the University Medical Center for customization of the DC stimulator as well as their technical support.

Appendix A. Supplementary data

Supplementary data to this article can be found online at https://doi.org/10.1016/j.brs.2019.07.026.

References

[1] Fritsch B, Reis J, Martinowich K, Schambra HM, Ji Y, Cohen LG, et al. Direct current stimulation promotes BDNF-dependent synaptic plasticity: potential implications for motor learning. Neuron 2010;66:198–204. https://doi.org/10.1016/j.neuron.2010.03.035.

[2] Sun Y, Lipton JO, Boyle LM, Madsen JR, Goldenberg MC, Pascual-Leone A, et al. Direct current stimulation induces mGluR5-dependent neocortical plasticity. Ann Neurol 2016;80:233–46. https://doi.org/10.1002/ana.24708.

[3] Reis J, Schambra HM, Cohen LG, Buch ER, Fritsch B, Zarahn E, et al. Noninvasive cortical stimulation enhances motor skill acquisition over multiple days through an effect on consolidation. Proc Natl Acad Sci 2009;106:1590–5. https://doi.org/10.1073/pnas.0805413106.

[4] Buch ER, Santarnecchi E, Antal A, Born J, Celnik PA, Classen J, et al. Effects of tDCS on motor learning and memory formation: a consensus and critical position paper. Clin Neurophysiol 2017;128:589–603. https://doi.org/10.1016/j.clinph.2017.01.004.

[5] Faraji J, Gomez-Palacio-Schjetnan A, Luczak A, Metz GA. Beyond the silence: bilateral somatosensory stimulation enhances skilled movement quality and neural density in intact behaving rats. Behav Brain Res 2013;253:78–89. https://doi.org/10.1016/j.bbr.2013.07.022.

[6] Rioult-Pedotti MS, Friedman D, Donoghue JP. Learning-induced LTP in neocortex. Science 2000;290:533–6. https://doi.org/10.1126/science.290.5491.533.

[7] Hodgson RA, Ji Z, Standish S, Boyd-Hodgson TE, Henderson AK, Racine RJ. Training-induced and electrically induced potentiation in the neocortex. Neurobiol Learn Mem 2005;83:22–32. https://doi.org/10.1016/j.nlm.2004.07.001.

[8] Monfils M-H, Teskey G. Skilled-learning-induced potentiation in rat sensorimotor cortex: a transient form of behavioural long-term potentiation. Neuroscience 2004;125:329–36. https://doi.org/10.1016/j.neuroscience.2004.01.048.

[9] Nabavi S, Fox R, Proulx CD, Lin JY, Tsien RY, Malinow R. Engineering a memory with LTD and LTP. Nature 2014;511:348–52. https://doi.org/10.1038/nature13294.

[10] Tsvetkov E, Carlezon WA, Benes FM, Kandel ER, Bolshakov VY. Fear conditioning occludes LTP-induced presynaptic enhancement of synaptic transmission in the cortical pathway to the lateral amygdala. Neuron 2002;34:289–300. https://doi.org/10.1016/S0896-6273(02)00645-1.

[11] Yuste R, Bonhoeffer T. Morphological changes in dendritic spines associated with long-term synaptic plasticity. Annu Rev Neurosci 2001;24:1071–89. https://doi.org/10.1146/annurev.neuro.24.1.1071.

[12] Holtmaat A, Svoboda K. Experience-dependent structural synaptic plasticity in the mammalian brain. Nat Rev Neurosci 2009;10:647–58. https://doi.org/10.1038/nrn2699.

[13] Engert F, Bonhoeffer T. Dendritic spine changes associated with hippocampal long-term synaptic plasticity. Nature 1999;399:66–70. https://doi.org/10.1038/19978.

[14] Xu T, Yu X, Perlik AJ, Tobin WF, Zweig JA, Tennant K, et al. Rapid formation and selective stabilization of synapses for enduring motor memories. Nature 2009;462:915–9. https://doi.org/10.1038/nature08389.

[15] Yang G, Pan F, Gan W-B. Stably maintained dendritic spines are associated with lifelong memories. Nature 2009;462:920–4. https://doi.org/10.1038/nature08577.

[16] Fu M, Yu X, Lu J, Zuo Y. Repetitive motor learning induces coordinated formation of clustered dendritic spines in vivo. Nature 2012;483:92–6. https://doi.org/10.1038/nature10844.

[17] Monfils M-H. Long-term potentiation induces expanded movement representations and dendritic hypertrophy in layer V of rat sensorimotor neocortex. Cerebr Cortex 2004;14:586–93. https://doi.org/10.1093/cercor/bhh020.

[18] Bourne J, Harris KM. Do thin spines learn to be mushroom spines that remember? Curr Opin Neurobiol 2007;17:381–6. https://doi.org/10.1016/j.conb.2007.04.009.

[19] Matsuzaki M, Honkura N, Ellis-Davies GCR, Kasai H. Structural basis of long-term potentiation in single dendritic spines. Nature 2004;429:761–6. https://doi.org/10.1038/nature02617.

[20] Matsuzaki M, Ellis-Davies GCR, Nemoto T, Miyashita Y, Iino M, Kasai H. Dendritic spine geometry is critical for AMPA receptor expression in hippocampal CA1 pyramidal neurons. Nat Neurosci 2001;4:1086–92. https://doi.org/10.1038/nn736.

[21] Paciello F, Podda MV, Rolesi R, Cocco S, Petrosini L, Troiani D, et al. Anodal transcranial direct current stimulation affects auditory cortex plasticity in normal-hearing and noise-exposed rats. Brain Stimul 2018;11:1008–23. https://doi.org/10.1016/j.brs.2018.05.017.

[22] Jiang T, Xu RX, Zhang AW, Di W, Xiao ZJ, Miao JY, et al. Effects of transcranial direct current stimulation on hemichannel pannexin-1 and neural plasticity in rat model of cerebral infarction. Neuroscience 2012;226:421–6. https://doi.org/10.1016/j.neuroscience.2012.09.035.

[23] Park H, Poo M. Neurotrophin regulation of neural circuit development and function. Nat Rev Neurosci 2013;14:7–23. https://doi.org/10.1038/nrn3379.

[24] Figurov A, Pozzo-Miller LD, Olafsson P, Wang T, Lu B. Regulation of synaptic responses to high-frequency stimulation and LTP by neurotrophins in the hippocampus. Nature 1996;381:706–9. https://doi.org/10.1038/381706a0.

[25] Kovalchuk Y. Postsynaptic induction of BDNF-mediated long-term potentiation. Science 2002;295:1729–34. https://doi.org/10.1126/science.1067766.

[26] Genoud C, Knott GW, Sakata K, Lu B, Welker E. Altered synapse formation in the adult somatosensory cortex of brain-derived neurotrophic factor heterozygote mice. J Neurosci 2004;24:2394–400. https://doi.org/10.1523/JNEUROSCI.4040-03.2004.

[27] Kellner Y, Gödecke N, Dierkes T, Thieme N, Zagrebelsky M, Korte M. The BDNF effects on dendritic spines of mature hippocampal neurons depend on neuronal activity. Front Synaptic Neurosci 2014;6:5. https://doi.org/10.3389/fnsyn.2014.00005.

[28] Podda MV, Cocco S, Mastrodonato A, Fusco S, Leone L, Barbati SA, et al. Anodal transcranial direct current stimulation boosts synaptic plasticity and memory in mice via epigenetic regulation of Bdnf expression. Sci Rep 2016;6:22180. https://doi.org/10.1038/srep22180.

[29] Feng G, Mellor RH, Bernstein M, Keller-Peck C, Nguyen QT, Wallace M, et al. Imaging neuronal subsets in transgenic mice expressing multiple spectral variants of GFP. Neuron 2000;28:41–51. https://doi.org/10.1016/S0896-6273(00)00084-2.
[30] Ernfors P, Lee K-FF, Jaenisch R. Mice lacking brain-derived neurotrophic factor develop with sensory deficits. Nature 1994;368:147–50. https://doi.org/10.1038/368147a0.
[31] Franklin KBJ, Paxinos G. The mouse brain in stereotaxic coordinates. New York: Academic Press; 2008.
[32] Gellner A-K, Reis J, Fritsch B. Glia: a neglected player in non-invasive direct current brain stimulation. Front Cell Neurosci 2016;10:188. https://doi.org/10.3389/fncel.2016.00188.
[33] Schindelin J, Arganda-Carreras I, Frise E, Kaynig V, Longair M, Pietzsch T, et al. Fiji: an open-source platform for biological-image analysis. Nat Methods 2012;9:676–82. https://doi.org/10.1038/nmeth.2019.
[34] Sage D, Donati L, Soulez F, Fortun D, Schmit G, Seitz A, et al. DeconvolutionLab2: an open-source software for deconvolution microscopy. Methods 2017;115:28–41. https://doi.org/10.1016/j.ymeth.2016.12.015.
[35] Holtmaat A, Bonhoeffer T, Chow DK, Chuckowree J, De Paola V, Hofer SB, et al. Long-term, high-resolution imaging in the mouse neocortex through a chronic cranial window. Nat Protoc 2009;4:1128–44. https://doi.org/10.1038/nprot.2009.89.
[36] Oray S, Majewska A, Sur M. Effects of synaptic activity on dendritic spine motility of developing cortical layer V pyramidal neurons. Cerebr Cortex 2006;16:730–41. https://doi.org/10.1093/cercor/bhj019.
[37] Kasai H, Matsuzaki M, Noguchi J, Yasumatsu N, Nakahara H. Structure–-stability–function relationships of dendritic spines. Trends Neurosci 2003;26:360–8. https://doi.org/10.1016/S0166-2236(03)00162-0.
[38] Rensing N, Ouyang Y, Yang XF, Yamada KA, Rothman SM, Wong M. In vivo imaging of dendritic spines during electrographic seizures. Ann Neurol 2005;58:888–98. https://doi.org/10.1002/ana.20658.
[39] Sigler A, Murphy TH. In vivo 2-photon imaging of fine structure in the rodent brain: before, during, and after stroke. Stroke 2010;41:S117–23. https://doi.org/10.1161/STROKEAHA.110.594648.
[40] Markram H, Lübke J, Frotscher M, Sakmann B. Regulation of synaptic efficacy by coincidence of postsynaptic APs and EPSPs. Science 1997;275:213–5.
[41] Bi G-Q, Poo M-M. Synaptic modifications in cultured hippocampal neurons: dependence on spike timing, synaptic strength, and postsynaptic cell type. J Neurosci 1998;18:10464–72. https://doi.org/10.1523/JNEUROSCI.18-24-10464.1998.
[42] Sanes JN, Donoghue JP. Plasticity and primary motor cortex. Annu Rev Neurosci 2000;23:393–415. https://doi.org/10.1146/annurev.neuro.23.1.393.
[43] Karni A, Meyer G, Rey-Hipolito C, Jezzard P, Adams MM, Turner R, et al. The acquisition of skilled motor performance: fast and slow experience-driven changes in primary motor cortex. Proc Natl Acad Sci 1998;95:861–8. https://doi.org/10.1073/pnas.95.3.861.
[44] Kleim JA, Barbay S, Nudo RJ. Functional reorganization of the rat motor cortex following motor skill learning. J Neurophysiol 1998;80:3321–5. https://doi.org/10.1152/jn.1998.80.6.3321.
[45] Tennant KA, Adkins DL, Scalco MD, Donlan NA, Asay AL, Thomas N, et al. Skill learning induced plasticity of motor cortical representations is time and age-dependent. Neurobiol Learn Mem 2012;98:291–302. https://doi.org/10.1016/j.nlm.2012.09.004.
[46] Clark TA, Fu M, Dunn AK, Zuo Y, Jones TA. Preferential stabilization of newly formed dendritic spines in motor cortex during manual skill learning predicts performance gains, but not memory endurance. Neurobiol Learn Mem 2018;152:50–60. https://doi.org/10.1016/j.nlm.2018.05.005.
[47] Kandel ER, Schwartz JH, Jessell TM, Siegelbaum SA, Hudspeth AJ. Principles of neural science. fifth ed., vol. 91. New York: McGraw-Hill Medica; 2013.
[48] Hering H, Sheng M. Dentritic spines : structure, dynamics and regulation. Nat Rev Neurosci 2001;2:880–8. https://doi.org/10.1038/35104061.
[49] Zuo Y, Lin A, Chang P, Gan W-B. Development of long-term dendritic spine stability in diverse regions of cerebral cortex. Neuron 2005;46:181–9. https://doi.org/10.1016/j.neuron.2005.04.001.
[50] Holtmaat AJGD, Trachtenberg JT, Wilbrecht L, Shepherd GM, Zhang X, Knott GW, et al. Transient and persistent dendritic spines in the neocortex in vivo. Neuron 2005;45:279–91. https://doi.org/10.1016/j.neuron.2005.01.003.
[51] Carretón O, Giralt A, Torres-Peraza JF, Brito V, Lucas JJ, Ginés S, et al. Age-dependent decline of motor neocortex but not hippocampal performance in heterozygous BDNF mice correlates with a decrease of cortical PSD-95 but an increase of hippocampal TrkB levels. Exp Neurol 2012;237:335–45. https://doi.org/10.1016/j.expneurol.2012.06.033.
[52] Korte M, Carroll P, Wolf E, Brem G, Thoenen H, Bonhoeffer T. Hippocampal long-term potentiation is impaired in mice lacking brain-derived neurotrophic factor. Proc Natl Acad Sci 1995;92:8856–60. https://doi.org/10.1073/pnas.92.19.8856.
[53] Zagrebelsky M, Korte M. Form follows function: BDNF and its involvement in sculpting the function and structure of synapses. Neuropharmacology 2014;76:628–38. https://doi.org/10.1016/j.neuropharm.2013.05.029.
[54] Chapleau CA, Pozzo-Miller L. Divergent roles of p75NTRand Trk receptors in BDNF's effects on dendritic spine density and morphology. Neural Plast 2012;2012:1–9. https://doi.org/10.1155/2012/578057.
[55] Chakravarthy S, Saiepour MH, Bence M, Perry S, Hartman R, Couey JJ, et al. Postsynaptic TrkB signaling has distinct roles in spine maintenance in adult visual cortex and hippocampus. Proc Natl Acad Sci 2006;103:1071–6. https://doi.org/10.1073/pnas.0506305103.
[56] Bartoletti A, Cancedda L, Reid SW, Tessarollo L, Porciatti V, Pizzorusso T, et al. Heterozygous knock-out mice for brain-derived neurotrophic factor show a pathway-specific impairment of long-term potentiation but normal critical period for monocular deprivation. J Neurosci 2018;22:10072–7. https://doi.org/10.1523/jneurosci.22-23-10072.2002.
[57] Zakharenko SS, Patterson SL, Dragatsis I, Zeitlin SO, Siegelbaum SA, Kandel ER, et al. Presynaptic BDNF required for a presynaptic but not postsynaptic component of LTP at hippocampal CA1-CA3 synapses. Neuron 2003;39:975–90. https://doi.org/10.1016/S0896-6273(03)00543-9.